IMPROVEMENT OF ADVANCED MICROWAVE SOUNDING UNIT TROPICAL CYCLONE INTENSITY AND SIZE ESTIMATION ALGORITHMS

Julie L. Demuth[1*]

Mark DeMaria[2]

John A. Knaff[1]

[1]Cooperative Institute for Research in the Atmosphere

Fort Collins, Colorado

[2]NOAA/NESDIS

Fort Collins, Colorado

Submitted to

Journal of Applied Meteorology

July 2005

**Corresponding author address*:

Julie L. Demuth

NCAR/ISSE

P.O. Box 3000

Boulder, CO 80307-3000

Phone: 303-497-8112; Fax: 303-497-8125

jdemuth@ucar.edu

Abstract

Previous work—in which Advanced Microwave Sounding Unit (AMSU) data from the Atlantic and east Pacific basins during 1999–2001 were used to provide objective estimates of 1-min maximum sustained surface winds, minimum sea level pressure, and the radii of 34-, 50-, and 64-kt (1 kt ≡ 0.5144 m s^{-1}) winds in the northeast, southeast, southwest, and northwest quadrants of tropical cyclones—is updated to reflect larger datasets, improved statistical analysis techniques, and improved estimation through dependent variable transforms. A multiple regression approach, which utilizes best-subset predictor selection and cross validation, is employed to develop the estimation models where the dependent data (i.e., maximum sustained winds, minimum pressure, wind radii) are from the extended best-track, and the independent data consist of AMSU-derived parameters that give information about retrieved pressure, winds, temperature, moisture, and satellite resolution. The developmental regression models result in mean absolute errors (MAE) of 10.8 kt and 7.8 hPa for estimating maximum winds and minimum pressure, respectively. The MAE for the 34-, 50-, and 64-kt azimuthally averaged wind radii are 16.9, 13.3, and 6.8 n mi (1 n mi ≡ 1.8519 km), respectively.

1. Introduction

The utility of satellite-based microwave remote sensing for observation and analysis of tropical cyclones (TC) has blossomed in the past decade because of the ability of microwave instruments to provide vertical profiles of TC parameters as well as useful details about the distribution of water vapor and deep convection. Moreover, the satellite-based data provide good global spatial coverage of the tropical regions. More details on the benefits of using microwave remote sensing for observing and analyzing TCs, including a brief description of several studies which do so, can be found in Demuth et al. 2004 (hereafter referred to as D04).

D04 capitalized on the efficacy of passive microwave remote sensing for observing TCs by using the Advanced Microwave Sounding Unit (AMSU), the follow-on to the Microwave Sounding Unit. For more details of the AMSU instrument and its use for TC applications, see Kidder et al. (2000), Knaff et al. (2000), Spencer and Braswell (2001), Brueske and Velden (2003), Knaff et al. (2004), and Bessho et al. (2006). D04 used AMSU-derived data from 1999–2001 to develop algorithms that provide objective estimates of intensity (i.e., 1-min maximum sustained winds [MSW] and minimum sea level pressure [MSLP]) and wind structure (i.e., radii of 34-, 50-, and 64-kt winds [1 kt ≡ 0.5144 m s^{-1}) for TCs in the Atlantic and East Pacific basins. The sample size consisted of 473 cases (i.e., passes over a TC) for the intensity estimation models and 129, 92, and 68 cases for the models estimating the 34-, 50-, and 64-kt wind radii, respectively.

The work by D04 has since been updated by developing a much larger, more representative, global set of data with TCs from the Atlantic, East Pacific, West Pacific, and Central Pacific basins as well as from the Indian Ocean and Southern Hemisphere. In addition, new potential estimative parameters were created based on transformations of original AMSU-

derived parameters. Finally, improved statistical model analysis and selection procedures were implemented to define the best possible estimation models. These modifications, improvements, and the resulting new models for estimating TC intensity and wind structure using AMSU data are described in the following sections. Only the necessary information and modifications are presented here, so the reader is referred to D04 for all the details of the methods not discussed in this follow-up.

2. Data and Methods

a. Data

The specifics of how the AMSU data are collected and processed and of the temperature and wind retrievals can be found in D04. For this work, data were collected from the AMSU instruments aboard the National Oceanic and Atmospheric Administration (NOAA)-15, -16, and -17 satellites. NOAA-15 data were available from 1999 through 2004, NOAA-16 data from 2001 through 2004, and NOAA-17 data from January through late October 2003. The NOAA-17 temperature profile data are unavailable after October 2003 because the AMSU-A instrument failed. Likewise, two stratospheric channels (i.e., Channels 11 and 14) have failed on the AMSU instrument aboard NOAA-15, but accommodating corrections to the temperature retrieval algorithm were made. The retrieval was limited to those cases in which the TC center fell within 700 km of the AMSU swath center. Previously, a threshold of 600 km was used, but that limit was increased to 700 km in order to increase the number of cases for testing. The increase of this threshold resulted in no degradation of these algorithms. This constraint resulted in AMSU cases being an average of less than 17 hours apart when only one NOAA satellite was available (during 1999 and 2000), 10–11.5 hours apart when two NOAA satellites were available (during

2001, 2002, and 2004), and approximately 8.5 hours apart when three NOAA satellites were available (during 2003).

In addition to D04's earlier work, in which the AMSU data were collected for all Atlantic and East Pacific TCs from 1999–2001, three more years of data (i.e., from 2002–04) were acquired, for a complete dataset ranging from 1999–2004. AMSU data also were collected for TCs in the Central Pacific and Indian Ocean from 2003–04, and in the West Pacific and Southern Hemisphere from 2002–04.

Acquisition of these new data results in 2637 and 2624 cases for estimating the MSW and MSLP, respectively, more than quintuple the size of D04's previous dataset for intensity estimation. The distribution of cases by basin (Figure 1) shows that approximately one-third of the cases are from the Atlantic basin, one-third are from the West Pacific basin, and the remaining one-third are from the other four basins combined. These new data provide 45 cases at the Category 5-level (> 135 kt) compared to D04, where there were no AMSU passes over a TC while it was of Category-5 intensity. As will be described in more detail in the next subsection, the new wind radii datasets were restricted to cases with coincident reconnaissance, leaving 255 cases for the 34-kt winds, 170 cases for the 50-kt winds, and 120 cases for the 64-kt winds. These recon-based sample sizes are nearly double the dataset from D04's previous work, in which the wind radii datasets were developed using only Atlantic cases west of 55°W—a restriction imposed because of the higher likelihood of having in situ measurements in that region—as well as Atlantic and East Pacific cases with reconnaissance.

b. Methods

The resolution of the AMSU data, which is 48 km at best, is too coarse to adequately resolve TC structure. Thus, parameters derived from the AMSU temperature, pressure, and wind retrievals are used to develop an empirically based statistical model for estimating TC intensity and winds in real time. As in D04's earlier work, 18 AMSU-derived parameters serve as potential estimators along with the 2 non-AMSU-derived parameters, latitude (LAT) and the operational estimate of intensity (VMXOP) (Table 1); the latter parameter—the operational estimate of TC intensity—is used only for estimating the wind radii. In addition to these 20 parameters, 4 additional estimators were added to the predictor pool (Table 1) to try to better estimate the stronger TCs—which the D04 algorithms typically do not estimate well because of the coarse horizontal resolution of the AMSU—and to better detect dissipating storms. Three of the new variables are transformations of other AMSU-derived variables. P600, or the surface pressure at a radius of 600 km, is not AMSU-derived; this information is determined from the National Centers for Environmental Prediction Global Forecast System model. P600 is used as a boundary condition for the AMSU pressure retrieval and, as such, is used to derive the minimum surface pressure (PMIN) and pressure drop at the surface (DP0), where P600=PMIN+DP0.

The dependent data for the TC intensity and wind radii estimations are from National Hurricane Center (NHC), Joint Typhoon Warning Center, and Central Pacific Hurricane Center extended best-track[1] data within 6 h of the AMSU swath time, linearly interpolated to the time of

[1] The extended best-track data supplements standard best-track position and intensity data—which are determined from post-season analyses of all information available and are reported every six hours—with operational estimates of TC size parameters (e.g., radii of 34-, 50-, and 64-kt winds, radius of maximum winds). The extended best track was prepared by Mark DeMaria with partial support from the Risk Prediction Initiative. Both the best track and the advisories containing wind-radii information used to create the extended best track come from the databases

the swath. The 34-, 50-, and 64-kt wind radii datasets were restricted to cases that had a reconnaissance flight within 12 hours prior, because estimates of the wind radii can be grossly in error when in situ observations are not available. The intensity datasets were not restricted to cases with coincident reconnaissance, because best-track estimates of intensities, unlike wind radii, are reasonably accurate and that doing so would have resulted in a much smaller set of cases. Of that smaller dataset, the vast majority of cases are from the Atlantic basin, only a handful are from the East Pacific and West Pacific basins, and there are no cases from the Central Pacific, Indian Ocean, or Southern Hemisphere. Thus, the much larger, more representative dataset is preferred.

1) INTENSITY ESTIMATION

Two algorithms are developed using AMSU data to estimate intensity, one each for the MSW and the MSLP. Again, in attempt to better estimate the stronger storms, the dependent data for both the MSW and MSLP were transformed in several ways. The results indicated that the MSW are best estimated directly, with the MSW values as the dependent data. However, the MSLP are best estimated indirectly; the data first are subtracted from a set value of 1050 hPa, then an algorithm to estimate the natural log of that differenced value is developed, and finally the MSLP is re-obtained.

To develop algorithms that estimate TC intensity, a best-subsets multiple linear regression (Miller, 2002) technique was employed. This technique examines all potential regression equation combinations up to some N number of variables. For example, if there were

---

maintained in the Automated Tropical Cyclone Forecast (Sampson and Schrader, 2000) databases at the National Hurricane Center and the Joint Typhoon Warning Center. Applications of the extended best track can be found in Kimball and Mulekar (2004).

three independent variables, the best-subsets technique would assess seven equations: three equations with single estimators, three equations with two estimators each, and one equation with all three estimators. The advantage of this method over an automated technique, such as stepwise regression, is that it allows the user to see the regression results from all possible models and to select the most appropriate model based on the user's criteria. The best-subsets technique was combined with a cross-validation scheme to provide a more realistic assessment of the errors. To thoroughly evaluate the models, the regression equations were developed with 80% of the cases, chosen randomly, and tested on the remaining 20% of the cases (Brieman and Spector, 1992). This 80/20 cross-validation procedure was conducted 1000 times for every possible model to ensure robust estimates of error.

To develop the intensity estimation models, best-subsets were used to analyze all possible models having up to 15 independent variables. The evaluation criteria included (1) the minimization of the mean absolute error (MAE)—which has the same units as the dependent variable so that there is physical meaning to the errors—of both the developmental and the cross-validated datasets, and (2) that all estimators are significant to 1% (α=0.01). Based on these results, the best models were chosen for estimating the MSW and MSLP.

2) Azimuthally Averaged and Asymmetric Wind Radii Estimation

As in D04's previous work, the azimuthally averaged wind radii of 34-, 50-, and 64-kt winds are estimated in a manner similar to the intensity estimation. The averaged wind radii values then were used in conjunction with a simple wind model—a modified Rankine vortex plus a vector proportional to TC motion—to estimate the asymmetric wind structure in terms of the wind radii in the northeast (NE), southeast (SE), southwest (SW), and northwest (NW)

quadrants of the TC. A complete discussion of the asymmetric wind radii estimation methods can be found in D04. The one difference, however, is that the dependent data for the azimuthally averaged dataset were established by averaging only the quadrants for which non-zero wind radii existed in the extended best-track data; previously, D04 took the average of all four quadrants, including those for which no wind radii existed. Eliminating the quadrants with zero wind radii from the average removes noise from the data for cases where the maximum wind is close to the 34-, 50-, or 64-kt wind radii threshold. In these cases, the wind radii in some quadrants rapidly vary between zero and non-zero values as a function of time.

The algorithms that estimate the azimuthally averaged 34-, 50-, and 64-kt wind radii are developed with the same methods as the intensity estimation algorithms—that is, with a best-subsets multiple linear regression combined with a cross-validation method that uses 80% of the data for developmental purposes and 20% of the data for testing, which is run 1000 times for each possible model. The evaluation criteria for the wind radii regressions are (1) the minimization of the MAE of the developmental and the cross-validated datasets, as with the intensity estimation models, and (2) that all estimators are significant to 5% (α=0.05). A less stringent significance level was used for the mean wind radii estimations than for the intensity estimations, because the smaller wind radii sample sizes made it difficult to achieve robust regression models with the more stringent significance level.

3. Intensity Estimation Results

The new regression equation for estimating MSW retains 12 variables and explains 78.7% of the variance (R^2), and an additional variable is retained for estimating MSLP,

explaining 80.2% of the variance (Table 2). Compared to D04, this is a 6.4% and 3.7% improvement in the R^2, respectively.

Seven parameters—DP0, TMAX, SS, RMX3, VBI5, CLWAVE, and CLWPER—defined the model used in D04 to estimate MSW and, with the addition of PMIN, to estimate MSLP. Those same seven variables are retained again, along with five additional variables (i.e., DP3, VMX3, VBO0, VBO3, and $TMAX^2$), to estimate MSW (Table 2). For the estimate of MSLP, the same original seven variables and five new variables are retained, but P600 now is retained in place of PMIN (Table 2). As discussed earlier, P600 is a model-derived boundary condition used to determine PMIN and DP0, where P600 is the sum of those two parameters; thus, any combination of two of these three variables provides the same information. P600 was chosen in place of PMIN—even though the developmental regression results are the same for either parameter—because it is easier to understand that P600 provides information about the background pressure environment than the combination of PMIN and DP0.

In Table 2, the normalized coefficients are indicative of the relative weight each variable has in providing the TC intensity estimates. For each variable, the normalized coefficients for the MSW and MSLP models have similar magnitudes. This similarity should be expected because, as described previously, the MSLP variable is actually the log of the difference in the central pressure from 1050 hPa, so a larger value of MSLP indicates a stronger storm, similar to MSW. The physical interpretation of the normalized coefficients in Table 2 is complicated by the fact that the variables can interact with each other. For example, DP0 and DP3 have the largest coefficients, but opposite signs. Thus, it is really the difference between these two variables that is correlated with the intensity. The direct relationship with intensity comes from the TMAX (modified by $TMAX^2$), VMX3 and VBI5 terms. A warmer core and stronger retrieved maximum

A-1

and average inner winds increase the intensity estimate. The effects of SS and RMX3 are smaller, but also have a direct physical interpretation. The intensity estimate in increased when SS is large (a correction for lower data resolution) and when RMX3 is smaller (more intense storms tend to have a smaller radius of maximum wind). The two moisture variables (CLWAVE and CLWPER) interact but increase the intensity when the CLW is generally higher. The remaining variables occur in pairs with opposite signs (DP0 with DP3 and VBO0 with VBO3) and are related to the vertical structure of the retrievals. These variables are probably providing additional corrections due to attenuation, which has a strong influence on the difference in the retrieved variables between vertical levels. The P600 variable increases the MSLP (which lowers the central pressure estimate) when the environmental pressure is low.

The MAE and rmse for the new MSW estimation model from the developmental dataset are 10.8 and 14.0 kt, respectively. For the new MSLP model, the MAE is 7.8 hPa and the rmse is 11.6 hPa. The errors stratified by TC intensity are given in Table 3. These data show that the AMSU intensity estimation algorithms work best on tropical storms (34–63 kt) and weak hurricanes (64–95 kt); they tend to overestimate the intensity of tropical depressions (< 34 kt); and they tend to underestimate the intensity of major hurricanes (≥ 96 kt), especially Category 5 storms (> 135 kt). Looking only at the MSW estimation, the model tends to underestimate MSW during instances of rapid intensification (defined here as at least 30 kt within 24 hr). This occurred 23 times, and the MAE of these cases is 23.4 kt with a bias of -20.2 kt. This may be due to a lag in the AMSU detecting changes in the warm core (i.e., TMAX) or that the warming in the core is distributed differently within rapidly intensifying storms.

B-4

An analysis of the errors for the MSW estimation stratified by the six basins and by intensity is shown in Table 4. The estimations for the Atlantic basin likely are of higher skill

B-2

because, of the 846 cases comprising the developmental dataset, 300 have coincident reconnaissance, resulting in a better developmental dataset. In comparison, it is possible that the larger errors for stronger hurricanes in the East Pacific, Southern Hemisphere, and West Pacific may be largely due to fewer in situ observations in these basins. There are also basin specific possibilities for these larger intensity errors. The East Pacific TCs are notably smaller than those in other basins (Knaff et al. 2006, manuscript submitted to *Wea. Forecasting*), and Southern Hemisphere positional errors are larger because forecast advisories are issued every 12 h in that region, as opposed to every 6 h. For the Central Pacific and Indian Ocean, the datasets are made up of very few cases, potentially making the error estimates less representative. For example, there was only one hurricane in the Indian Ocean, so the 29.7 kt error shown in Table 4 is based on this case alone.

When comparing the error statistics from the new intensity estimation models with those from D04, on the surface it appears as though the new models result in slightly greater errors (Table 5). However, testing the intensity estimation models from D04 on the new, more representative datasets provides a more direct assessment of the errors. Applying the MSW model from D04 to the new data results in MAE and rmse of 11.5 and 14.8 kt (Table 5) and applying the MSLP model results in errors of 8.9 and 13.1 hPa (not shown in Table 5), all of which are higher than the errors from the new models. These results are consistent when examining the errors stratified by TC intensity. A specific analysis of the Category 5 storms shows that the D04 model estimates of MSW are in error by an average of 4 kt more than the new MSW model estimate (MSLP by 15 hPa; not shown). Thus, the new intensity estimation models are better overall than the D04 models, and they are especially better at estimating

stronger TCs, in part because the new datasets include several cases of Category-5 intensity, whereas the D04 dataset had none.

4. Wind Radii Estimation Results

a. Azimuthally averaged wind radii

Unlike the updated intensity estimation models, which employed all of the same estimative parameters as in D04, the revised azimuthally averaged wind radii estimation models differ considerably from the old versions. This probably is due to the previous datasets being less representative because of their smaller sample sizes and their not being comprised solely of cases coincident with reconnaissance data to ensure more accurate observations. As such, the new models are more robust, as is shown by their improved error statistics.

The final regression equations for the 34- and 50-kt mean wind radii each retain 10 variables, and the 64-kt mean wind radii equation retains 9 variables (Table 6). The normalized coefficients for the wind radii are more difficult to interpret physically than those for the intensity estimation because there is more interaction among the independent variables. The SS and RMX0 variables have a direct relationship, increasing the radii for large SS (resolution correction) and when RMX0 is large. The radii also increase for larger TMAX, although there is some interaction with CLWAVE for the 34-kt radii. This relationship probably represents the increase in storm radii when the storm becomes more intense. For the 50-kt radii, the combination of the VMXOP and TMAX terms represents this same effect. For the 64-kt radii, larger CLWPER values are related to larger radii; this might be expected, because larger storms tend to have larger cloud regions. The relationship with the CLW variables is more difficult to interpret for the 34- and 50-kt winds, because there is considerable interaction with other terms.

A-1

Similar to the intensity coefficients, there are several variables that have similar coefficients but opposite signs, which probably is related to attenuation effects.

The mean 34-kt algorithm explains 78.4% of the variance, and it results in a MAE of 16.9 n mi and a rmse of 21.4 n mi (1 n mi ≡ 1.8519 km). For the mean 50-kt wind radii, 78.2% of the variance is explained, and the MAE and rmse are 13.3 and 17.3 n mi, respectively. Finally, the mean 64-kt wind radii algorithm explains 86.4% of the variance and results in MAE and rmse of 6.8 and 8.9 n mi, respectively. The improved errors from the updated models compared to the models from D04 are shown in Table 7.

b. Asymmetric wind radii

The improved azimuthally averaged wind radii estimates lead to improved estimates of the wind radii in the NE, SE, SW, and NW quadrants of the TC. Figure 2 shows the MAE of each wind radii by quadrant based on the revised models and the D04 models. Although there are only slight improvements in the NE quadrant—which averages the largest wind radii of all four quadrants for all three wind thresholds—the radii in the other three quadrants improve substantially.

5. Summary and Conclusions

This research was a follow-on to previous work conducted by Demuth et al. (2004) to improve the estimation of tropical cyclone intensity (i.e., in terms of the maximum sustained winds and minimum sea level pressure) and wind structure (i.e., in terms of the radii of 34-, 50-, and 64-kt winds in the northeast, southeast, southwest, and northwest quadrants of the storm) using parameters derived from AMSU data. In their original work, Demuth et al. only had data

from tropical cyclones in the Atlantic and East Pacific basins from 1999 through 2001 on which to develop their algorithms. An additional 3 years of data, as well as data from tropical cyclones in the Central and West Pacific basins, Indian Ocean, and Southern Hemisphere, provide a much larger and more representative sample set. The added data more than quintupled the prior dataset for intensity estimation. The mean wind radii datasets, which are twice as large as before, are based entirely on cases coincident with aircraft reconnaissance within 12 hours prior. Moreover, the mean wind radii were calculated without averaging quadrants with zero wind radii, improving the mean radii estimates which, in turn, improves the asymmetric wind estimates. The intensity and azimuthally averaged wind structure estimation models were developed using a best-subsets technique, which analyzes all possible combinations of up to 15 independent variables. Every model was cross-validated 1000 times by using 80% of the cases, randomly chosen, for development and using the remaining 20% of the cases for testing. Overall, the larger datasets and modified methods result in superior estimates of intensity, especially for stronger TCs, and wind structure when compared to D04.

These revised algorithms were transitioned to operations at the National Hurricane Center/ Tropical Prediction Center (NHC/TPC) during 2005, where they will provide objective, and independent TC intensity estimates. The results generated at NHC will be provided to all U.S. operational tropical cyclone forecast centers using data from the NOAA-15, -16, and -18 satellites. Currently, there are no plans to revise these algorithms further using AMSU data. However, a new NOAA satellite system, NPOESS (National Polar-orbiting Operational Environmental Satellite System), is slated for launch in 2009. On NPOESS will be the Cross-track Infrared Sounder (CrIS) and the Advanced Technology Microwave Sounder (ATMS).

Denoted jointly as CrIMSS, this sensor suite will provide global profiles of temperature, moisture, and pressure, which could be used for future TC applications.

Acknowledgements. This research was funded by NOAA Grant NA17RJ1228. Views, opinions, and findings in this paper are those of the authors and should not be construed as an official NOAA and/or U.S. Government position, policy, or decision.

References

Bessho, K., M. DeMaria, and J. A. Knaff, 2006: Tropical cyclone wind retrievals from the Advanced Microwave Sounding Unit: Application to surface wind analysis. *J. Appl. Meteor.*, in press.

Brieman, L. and P. Spector, 1992: Submodel selection and evaluation in regression: The X-random case. *Int. Statist. Rev.*, **60**, 291–319.

Brueske, K. F. and C. S. Velden, 2003: Satellite-based tropical cyclone intensity estimation using the NOAA-KLM series Advanced Microwave Sounding Unit (AMSU). *Mon. Wea. Rev,* **131,** 687–697.

Demuth, J. L., M. DeMaria, J. A. Knaff, and T. H. Vonder Haar, 2004: Evaluation of Advanced Microwave Sounding Unit tropical-cyclone intensity and size estimation algorithms. *J. Appl. Meteor.*, **43**, 282–296.

Kidder, S. Q., M. D. Goldberg, R. M. Zehr, M. DeMaria, J. F. W. Purdom, C. S. Velden, N. C. Grody, and S. J. Kusselson, 2000: Satellite analysis of tropical cyclones using the Advanced Microwave Sounding Unit (AMSU). *Bull. Amer. Meteor. Soc.*, **81**, 1241–1259.

Kimball, S. K. and M. S. Mulekar. 2004: A 15-Year climatology of North Atlantic tropical cyclones. Part I: Size parameters. *J. Climate*, **17**, 3555–3575.

Knaff, J. A., R. M. Zehr, M. D. Goldberg, and S. Q. Kidder, 2000: An example of temperature structure differences in two cyclone systems derived from the Advanced Microwave Sounding Unit. *Wea. Forecasting*, **15**, 476–483.

-----, S. A. Seseske, M. DeMaria, and J. L. Demuth, 2004: On the influences of vertical wind shear on symmetric tropical cyclone structure derived from AMSU. *Mon. Wea. Rev.*, **132**, 2503–2510.

Miller, A. J., 2002: *Subset Selection in Regression, Second Edition*. Chapman and Hall, 238.

Sampson, C. R. and A. J. Schrader, 2000: The automated tropical cyclone forecasting system (Version 3.2). *Bull. Amer. Meteor. Soc*., **81**, 1131-1240.

Spencer, R. W. and W. D. Braswell, 2001: Atlantic tropical cyclone monitoring with AMSU-A: Estimation of maximum sustained wind speeds. *Mon. Wea. Rev.*, **129**, 1518–1532.

Figure 1. Distribution of tropical cyclone cases by basin for the intensity estimation datasets. Shown is the dataset for MSW, with n=2637 cases. For MSLP, with n=2624 cases, only the Atlantic and east Pacific distributions are different, with 31.9% and 25.2%, respectively.

Figure 2. Comparison of MAE for asymmetric 34-, 50-, and 64-kt wind radii between revised algorithms (new) and D04 algorithms (old). The concentric circles represent increasing error from the center of the graph at five-n mi increments.

Table 1. Potential estimators of tropical cyclone intensity and wind radii. The radius is denoted by r, where r=0 km is the storm center, and z is height. Except for the area-averaged CLWPER, all AMSU-derived parameters are azimuthally averaged.

Table 2. Regression variables and statistics for estimating MSW (kt) and MSLP (hPa). For all the independent variables, the p-value = 0.00000. The seven variables in **bold** were used to estimate MSW and MSLP in D04. The other variable used to estimate MSLP in D04 was the AMSU-derived minimum pressure (PMIN), which is replaced here by P600.

A-2

Table 3. Error statistics for the estimates of MSW and MSLP, stratified by tropical cyclone intensity. The statistics for the hurricane-strength storms are shown all together, and stratified by the categorical intensity based on the Saffir-Simpson scale.

B-3

Table 4. Mean absolute error statistics [kt] for the estimates of MSW, stratified by tropical cyclone intensity and by basin.

Table 5. Comparison of model performance for estimating MSW (kt) among the D04 model (old model) applied to the D04 developmental data set (old data), the D04 model applied to the revised dataset (new data), and the revised model (new model) applied to the revised dataset. Errors are shown for the whole datasets and stratified by tropical cyclone intensity. The errors for all hurricane-strength storms are shown as well as the errors specifically for the Category 5 storms.

Table 6. Regression variables and statistics for estimating the azimuthally averaged radii of 34-, 50-, and 64-kt winds (n mi). The variables in **bold** were used to estimate the wind radii in D04.*

Table 7. Comparison of variance explained (R2) and error statistics (MAE and rmse) for azimuthally averaged 34-, 50-, and 64-kt wind radii between revised algorithms (new model) and D04 algorithms (old model).

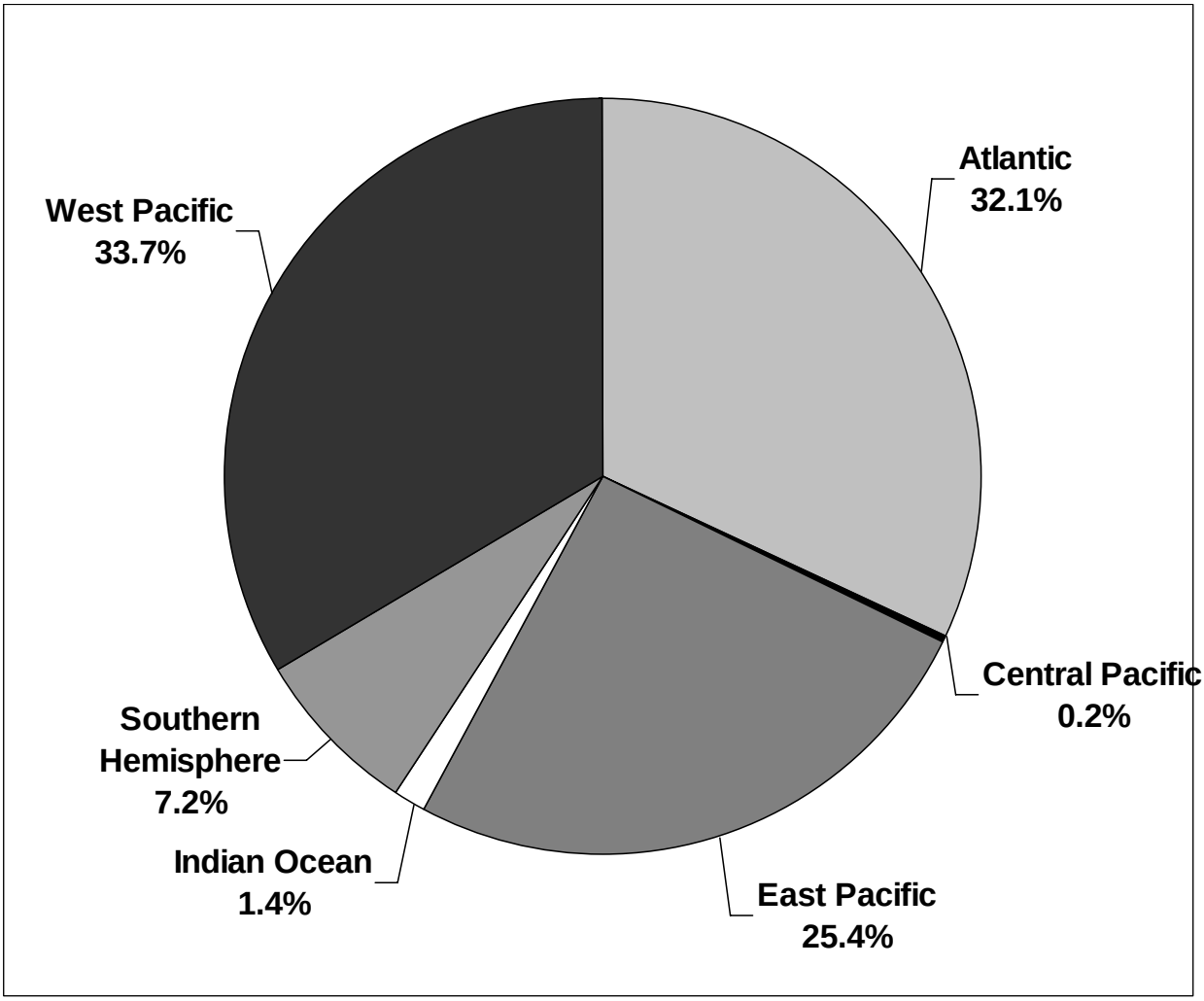

Figure 1. Distribution of tropical cyclone cases by basin for the intensity estimation datasets. Shown is the dataset for MSW, with n=2637 cases. For MSLP, with n=2624 cases, only the Atlantic and east Pacific distributions are different, with 31.9% and 25.2%, respectively.

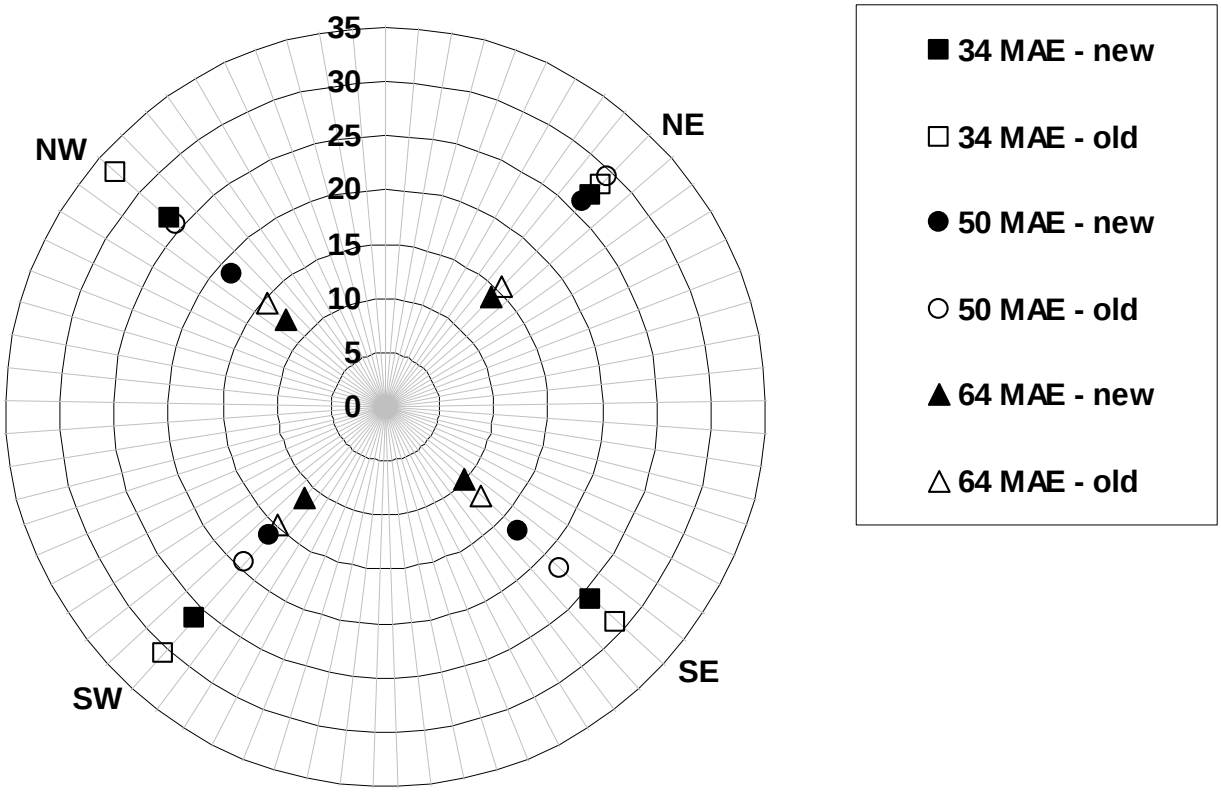

Figure 2. Comparison of MAE (n mi) for asymmetric 34-, 50-, and 64-kt wind radii between revised algorithms (new) and D04 algorithms (old). The concentric circles represent increasing error from the center of the graph at five-n mi increments.

Table 1. Potential estimators of tropical cyclone intensity and wind radii. The radius is denoted by r, where r=0 km is the storm center, and z is height. Except for the area-averaged CLWPER, all AMSU-derived parameters are azimuthally averaged.

Acronym	Description
	20 original potential estimators
PMIN	Min surface pressure (hPa) at storm center
DP0	Pressure drop (hPa) at surface from r=600 to 0 km
DP3	Pressure drop (hPa) at z=3 km from r=600 to 0 km
TMAX	Maximum temperature perturbation (°C) calculated as the temperature at r=600 km minus the temperature at each radius
ZMAX	Height (km) of maximum temperature perturbation (TMAX)
SS	Cross-track resolution (km) of AMSU footprint at storm center
VMX0	Maximum wind speed (kt) at surface
RMX0	Radius (km) of maximum winds at surface
VMX3	Maximum wind speed (kt) at z=3 km
RMX3	Radius (km) of maximum winds at z=3 km
VBI0	Tangential winds at surface, averaged from r=0 to 250 km
VBI3	Tangential winds at z=3 km, averaged from r=0 to 250 km
VBI5	Tangential winds at z=5 km, averaged from r=0 to 250 km
VBO0	Tangential winds at surface, averaged from r=250 to 500 km
VBO3	Tangential winds at z=3 km, averaged from r=250 to 500 km
VBO5	Tangential winds at z=5 km, averaged from r=250 to 500 km
CLWAVE	CLW content (mm), averaged from r=0 to 100 km
CLWPER	Percentage of area with CLW values > 0.5 mm from r=0 to 300 km

LAT*	Latitude from NHC at storm center, interpolated to AMSU swath time
VMXOP*	Operational estimate of maximum sustained winds (kt) from NHC
	4 new potential estimators
$TMAX^2$	The squared value of the maximum temperature perturbation (TMAX)
TMAX*CLWAVE	The maximum temperature perturbation (TMAX) times the squared value of the CLW content (CLWAVE)
$CLWAVE^2$	The squared value of the CLW content (CLWAVE)
P600*	Surface pressure (hPa) at r=600, the edge of the analysis domain

*These parameters are not derived from AMSU data.

A-2

Table 2. Regression variables and statistics for estimating MSW (kt) and MSLP (hPa). For all the independent variables, the p-value = 0.00000. The seven variables in **bold** were used to estimate MSW and MSLP in D04. The other variable used to estimate MSLP in D04 was the AMSU-derived minimum pressure (PMIN), which is replaced here by P600.

Independent variable	Maximum sustained winds (kt) R^2 = 78.7%, n=2637		Minimum sea level pressure (hPa) R^2 = 80.2%, n=2624	
	Coef	Normalized coef	Coef	Normalized coef
DP0	-4.33459	-1.11082	-0.04260	-0.97065
DP3	6.48789	1.12637	0.06316	0.97499
TMAX	6.28701	0.43377	0.07395	0.45339
SS	0.13380	0.05446	0.00153	0.05553
VMX3	0.49635	0.26216	0.00537	0.25166
RMX3	-0.02713	-0.08288	-0.00029	-0.07767
VBI5	1.72608	0.37544	0.01681	0.32463
VBO0	1.85672	0.42698	0.01753	0.35812
VBO3	-2.48450	-0.50946	-0.02156	-0.39237
CLWAVE	19.84888	0.32547	0.20820	0.30325
CLWPER	-0.26614	-0.20932	-0.00209	-0.14620
$TMAX^2$	-0.51428	-0.30871	-0.00655	-0.34972
P600	----	----	-0.01145	-0.14391

Table 3. Error statistics for the estimates of MSW and MSLP, stratified by tropical cyclone intensity. The statistics for the hurricane-strength storms are shown all together, and stratified by the categorical intensity based on the Saffir-Simpson scale.

B-3

	MSW			MSLP		
	MAE	RMSE	Bias*	MAE	RMSE	Bias*
Tropical depressions (< 34 kt) (MSW: n=686; MSLP: n=675)	9.2	11.5	7.7	4.8	6.1	-3.3
Tropical storms (34–63 kt) (MSW: n=1083; MSLP: n=1084)	9.6	12.0	0.1	5.7	7.6	-0.5
All hurricanes (≥ 64 kt) (MSW: n=868; MSLP: n=865)	13.6	17.7	-6.2	12.7	17.4	6.2
Category 1 (64–82 kt) (MSW: n=322; MSLP: n=316)	11.7	14.7	-0.1	9.4	12.3	0.2
Category 2 (83–95 kt) (MSW: n=164; MSLP: n=165)	11.7	14.8	-3.4	10.4	13.3	2.8
Category 3 (96–113 kt) (MSW: n=185; MSLP: n=187)	12.5	17.5	-7.4	12.2	17.1	7.5
Category 4 (114–135 kt) (MSW: n=152; MSLP: n=152)	16.6	21.2	-14.4	17.5	21.8	13.7
Category 5 (> 135 kt) (MSW: n=45; MSLP: n=45)	27.4	31.7	-27.4	30.7	36.3	30.1

*Bias is the average estimated values minus the average observed values. For MSW, a positive bias means the intensity was overestimated; for MSLP, a positive bias means the intensity was underestimated.

Table 4. Mean absolute error statistics [kt] for the estimates of MSW, stratified by tropical cyclone intensity and by basin.

	Atlantic	Central Pacific	East Pacific	Indian Ocean	Southern Hemisphere	West Pacific
Tropical depressions (< 34 kt)	7.8	9.7	9.3	15.8	13.7	9.4
Tropical storms (34–63 kt)	8.8		8.8	9.5	13.4	10.3
Category 1 (64–82 kt)	10.7		14.2	29.7	12.8	11.2
Category 2 (83–95 kt)	8.3		14.2		11.0	13.2
Category 3 (96–113 kt)	9.2		18.0		17.9	11.8
Category 4 (114–135 kt)	13.8		32.1		20.8	13.7
Category 5 (> 135 kt)	16.2		32.5		31.8	29.7

Table 5. Comparison of model performance for estimating MSW (kt) among the D04 model (old model) applied to the D04 developmental data set (old data), the D04 model applied to the revised dataset (new data), and the revised model (new model) applied to the revised dataset. Errors are shown for the whole datasets and stratified by tropical cyclone intensity. The errors for all hurricane-strength storms are shown as well as the errors specifically for the Category 5 storms.

	Old model on old data		Old model on new data		New model on new data	
	MAE	RMSE	MAE	RMSE	MAE	RMSE
All tropical cyclones	10.6	13.5	11.5	14.8	10.8	14.0
Tropical depressions (< 34 kt)	9.6	11.8	10.3	12.9	9.2	11.5
Tropical storms (34–63 kt)	9.1	11.4	10.5	13.0	9.6	12.0
All hurricanes (≥ 64 kt)	13.3	17.0	13.7	17.9	13.6	17.7
Category 5 (> 135 kt)	----	----	31.3	35.0	27.4	31.7

Table 6. Regression variables and statistics for estimating the azimuthally averaged radii of 34-, 50-, and 64-kt winds (n mi). The variables in **bold** were used to estimate the wind radii in D04.*

Independent variable	Coef	Normalized coef	p-value
Azimuthally averaged 34-kt wind radii (n mi) R^2 = 78.4%, n=255			
PMIN	-1.67423	-0.37416	0.00046
DP0	3.46238	0.69620	0.00000
TMAX	10.41016	0.57868	0.00088
SS	0.38938	0.09591	0.00422
VMX0	-0.67877	-0.27736	0.00651
RMX0	0.09078	0.17946	0.00000
CLWAVE	-39.64186	-0.43684	0.00754
CLWPER	0.30049	0.13851	0.02238
TMAX*CLWAVE	-8.81319	-0.94982	0.00003
$CLWAVE^2$	30.62560	0.75196	0.00084
Azimuthally averaged 50-kt wind radii (n mi) R^2 = 78.2%, n=170			
DP0	2.56301	0.66179	0.00002
TMAX	6.85088	0.47242	0.00292
VMX0	0.89570	0.44740	0.03951
RMX0	0.06395	0.14058	0.00219
VBI0	-5.54525	-1.15423	0.01145
VBI3	13.59224	2.61995	0.01456
VBI5	-13.04493	-2.41642	0.00150
CLWAVE	-18.61025	-0.23377	0.00151

CLWPER	0.27442	0.14557	0.02718
VMXOP	0.49101	0.36035	0.00002
Azimuthally averaged 64-kt wind radii (n mi) R^2 = 86.4%, n=120			
SS	0.37589	0.17091	0.00001
VMX0	2.10560	1.47816	0.00000
VMX3	-2.52543	-1.62224	0.00009
VBI0	-4.11899	-1.16041	0.00245
VBI3	6.62236	1.65812	0.00209
VBO3	1.75455	0.44403	0.02299
VBO5	-1.94906	-0.43220	0.05254
CLWPER	0.15221	0.11310	0.03941
$TMAX^2$	0.45719	0.51378	0.00000

*Variables in the mean wind radii models from D04 that are not in the revised models are: for 34-kt, VBI5, LAT, and VMXOP; for 50-kt, VMX3 and VBO5; for 64-kt, TMAX and VMXOP.

Table 7. Comparison of variance explained (R^2) and error statistics (MAE and rmse) for azimuthally averaged 34-, 50-, and 64-kt wind radii between revised algorithms (new model) and D04 algorithms (old model).

	Azimuthally averaged 34-kt wind radii		Azimuthally averaged 50-kt wind radii		Azimuthally averaged 64-kt wind radii	
	New model	Old model	New model	Old model	New model	Old model
R^2	78.4%	71.9%	78.2%	65.9%	86.4%	80.8%
MAE	16.9	21.2	13.3	17.9	6.8	8.0
Rmse	21.4	28.3	17.3	23.3	8.9	10.1